

Four-Dimensional Field of Light and Shadow: A New State of Light

Simon Rivera¹

¹ Air Force Retiree, Martinique, France

Correspondence: Simon Rivera, Air Force Retiree, Martinique, France. E-mail: fls.exp@yahoo.com

Received: March 10, 2025

Accepted: April 16, 2025

Online Published: April 27, 2025

doi:10.5539/apr.v17n1p147

URL: <https://doi.org/10.5539/apr.v17n1p147>

Abstract

The concept of a light source capable of directly exhibiting the spatial characteristics of a photon within observed reality—without reliance on instrumentation—has been previously considered and subsequently dismissed due to the complexity of its implementation. However, this discovery demonstrates that a specific type of light source allows such validation. When this nearly spherical light source—composed of vertical bands—diffuses its brightness throughout a room, bright and dark vertical fringes are visible on a screen inside a box equipped with a vertical slit. Notably, when the source is tilted, these fringes remain vertical, indicating the presence of a field that interacts with space. Introducing a three-dimensional coordinate system onto the fringe screen reveals inconsistencies as the inclination of the source changes. These inconsistencies stem from the overlapping trajectories of nearby fringes, which occupy mutually incompatible spatial positions. To resolve this, the geometry of the fringe screen must be constrained such that only one dimension is defined, with two distinct color states. Through the application of geometry links between physical parameters, these two color states necessitate a method for constructing a valid four-dimensional Euclidean coordinate system. This new system represents an advancement over the conventional four-dimensional **R**-vector space by explicitly defining the fourth dimension. Within the four-dimensional reality of the box, it becomes possible to derive the full geometric characteristics of an observable photon, as well as a discontinuity in the direct propagation of light and shadow through space.

Keywords: 4d, experience, source, light, shadow, fringe, fourth dimension, Photon's form, discontinuous propagation, four-dimensional vector space, euclidean, field, box, slit, Cartesian Coordinate System, experiment, corpuscular theory

1. The Bright and Dark Fringes

The light source consists of a vertical band cover in the shape of a sectioned sphere of precise dimensions, equipped with a halogen bulb that has either one or two vertical filaments at its center Figure 1. This setup produces vertical light beams and shadow volumes. The source is suspended by its power cable in a room where a box, approximately 60 cm on each side, is positioned Figure 2. The box has a screen and a vertical slit, a few millimeters wide, positioned such that the slit is located 7 meters from the corner of the room, aligning the center of the screen, the slit, and the corner Figure 3. Initially, vertical and straight bright and dark fringes can be observed inside the box, extending from the top to the bottom of the screen Figure 4. These fringes form because the vertical light beams and shadow volumes are sectioned by the slit. The phenomenon becomes particularly intriguing when the light source is pushed in any direction to induce large oscillatory movements, while avoiding rotation around its own axis. Despite these oscillations, the fringes remain vertical and distinct Figure 5, with only minimal horizontal movement on either side of a vertical axis positioned at the center of the screen. This makes the effect visually striking. When a larger box is used, the fringes appear even more impressive, as they extend higher while remaining vertical, distinct, and straight. However, with a larger box, the fringes exhibit significant lateral movement at the left and right edges of the image when the source oscillates. This is why a box of approximately 60 cm per side is preferred—it defines a 3d space where horizontal movement remains minimal throughout, creating a well-delimited space that simplifies analysis.



Figure 1. The light source consists of a spherical structure with a diameter of 29.5 cm, sectioned at the bottom. It is composed of 42 vertical bands, each with an average width of 1.26 cm, which create 42 slits with an average width of 0.95 cm at mid-height. The structure can accommodate a bulb positioned at its center, featuring either one or two vertical filaments



Figure 2. The box used has approximate dimensions of 60 cm × 60 cm × 60 cm. A box with slightly greater depth between the slit and the screen and/or increased height can also be used. However, it is preferable to limit the width to ensure that the horizontal movement of the fringes on the screen remains minimal throughout. On one side of the box, there is a tall vertical slit, and positioned in front of it is a white screen

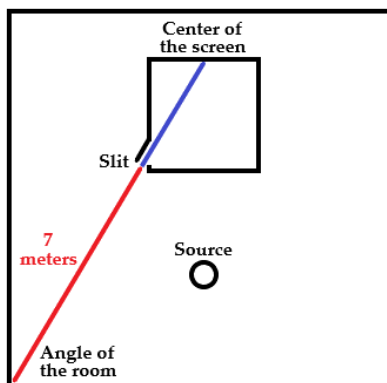


Figure 3. Top-View Positioning of the Box (Not to Scale). The center of the screen, the slit, and the corner of the room are aligned. To achieve a regular image, a minimum distance of 6.50 meters must be maintained between the slit and the corner of the room

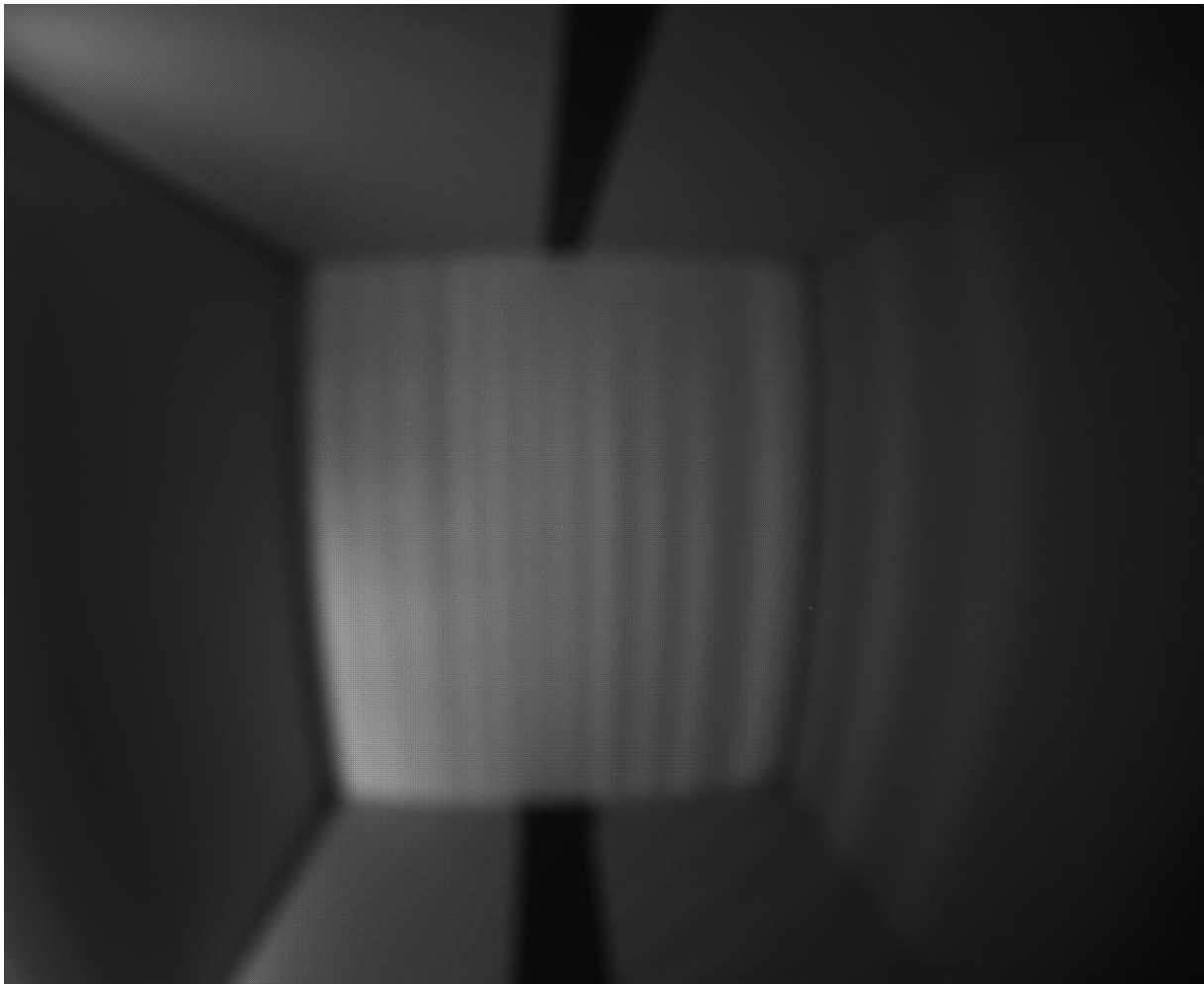


Figure 4. Photograph of the Fringes Captured with an Astronomy Camera. To enhance brightness, the slit is positioned 5.50 meters from the corner of the room instead of the standard 7 meters. The light source used has a single filament. When a two-filament bulb is used, the fringes appear slightly more pronounced but less sharply defined



Figure 5. If the light source remains inclined—similar to a freeze-frame capturing the oscillation motion—the astronomy camera photographs the vertical and straight fringes inside the box. These fringes appear in blue when observed on the computer screen. The distance between the slit and the corner of the room is 5.50 meters

2. The Field

Since the diffraction phenomenon is not considered at the slit—given that the slit is wide compared to the wavelength—and diffraction at the slit edges is not observed, we should, in principle, be able to apply the concept of geometric optics in reverse. This would allow us to reconstruct the images of reflections on the walls of the room facing the slit by tracing back from the fringe patterns. However, the distinct pattern of vertical fringes introduces a constraint: under reverse reconstruction, we would expect to observe vertical bands on these walls. Yet, when the source is inclined, we instead observe highly tilted bands—or, in some cases, no bands at all—depending on whether the downward projected conical beam from the source illuminates them. This indicates that reverse tracing fails. Moreover, since the real images of the inclined bands on the walls are observed in the room and reach the slit in straight lines, and given that the vertically sectioned beams inside the box allow for tracing of light rays in straight lines, it becomes impossible to maintain straight-line tracing at the slit itself. This confirms a definite break in geometric optics at the position of the slit, as shadow projections also do not follow straight-line paths. Taking this rupture into account, along with the regularity of the 2d horizontal movement of light beams and shadow volumes inside the box, we recognize the presence of a field that interacts with space. We refer to this as the “field of light and shadow”.

3. 4 Dimensions of Real Space to Explain the Phenomenon

A dimension refers to a line whose geometric content describes continuous real space. A dimension that is “emptied of its geometric content” remains valid in Euclidean space, provided that its parameters are adapted to continuous real space.

To better understand the space influenced by the field, we establish within both the supposed Galilean reference frame of the experiment room and Euclidean space, a right-handed 3d orthogonal coordinate system (x, y, z) of oriented Euclidean vector space of center O with “x” in slit-screen dimension, “y” the horizontal dimension positioned on the screen of the fringes and “z” the vertical dimension. Although geometric optics cannot be applied at the slit level, we rely on the fact that the observed fringes correspond to the image of the banded cover of the source. This means that each fringe on the screen originates from a specific volume of light or shadow in the room. Let P_n be a fixed point within a numbered source n, and let F_n be the transformed point of P_n, located on the fringe numbered n and corresponding to that volume. During a full oscillatory movement of the source in a given direction, if dzP_n is the vertical component of the small displacement \overline{dPn} of the point P_n, and if \overline{dFn} is the small rectilinear horizontal displacement observed of the point F_n, T_{3n} being the transformation which transforms dzP_n into dzF_n, dzP_n is the solution to the displacement equation dzF_n of \overline{dFn} :

$$\overline{dPn} \begin{cases} dxPn \\ dyPn \\ dzPn \end{cases} \quad \overline{dFn} \begin{cases} dxFn = T1n (dxPn) \\ dyFn = T2n (dyPn) \\ dzFn = T3n (dzPn) \end{cases}$$

When dzP_n occurs continuously within the vertical space z_n of the “z” axis, which corresponds to the room height h, i.e. z_n = h, the observed displacement dzF_n along the entire horizontal trajectory of fringe n takes place within this transformed vertical space, where z_n = h transformed:

$$z \text{ fringe } n = T3n (zn) = T3n (h)$$

This means that fringe n travels through the transformed vertical space of the room height, denoted as T_{3n} (h) along its horizontal trajectory. In the transformation from one point to another, a single transformed point on “y” cannot correspond to multiple untransformed points at different heights. When different offset fringe trajectories overlap on “y”, the “y” axis perceives “z” as containing multiple spatial positions of “z” at the same point of “z”. This results in a deformation of the geometric content that is supposed to represent continuous real space. Meanwhile, “z” itself remains consistent, as it correctly locates the source volumes at a single height h. However, this means that “z” is actually invalidated, as is the entire 3d coordinate system. We define the length on “y” where two different fringe trajectories overlap as “incompatible space”. The screen geometry of the fringes directly determines the exact number of additional dimensions required to be positioned coincident with “y”. We know the number of incompatible spaces at a given location on “y” because it corresponds to the number of different fringe trajectories which overlap at that point with a fringe trajectory already positioned on “y”. This number also corresponds to the number of dimensions to position in addition to “y” on the screen to separate these trajectories and eliminate incompatible spaces. In a large box, there is at least one incompatible space to the left and right of each fringe – sometimes even two or three – at the edges of the image, where the fringes have more horizontal movement. This corresponds to the need for at least one additional dimension on the screen. However, given the limited horizontal movement of the fringes observed with the preferred box size, only a maximum of one additional dimension is required—sufficient to eliminate the incompatible spaces located to the

left and right of each fringe. As a result, we need to position exactly one dimension on the screen, and this dimension has two possible colour states. That is, either the trajectories of the dark fringes are assigned to this additional dimension while the bright fringes remain on “y”, or vice versa Figure 6. This extra dimension is necessary not only for a specific direction of oscillatory motion but for all possible push directions across the full 360 ° range. Since the movement of the fringes remains weak, this confirms that the field is well-structured and stable at any point in the room. In the transition to 4d, we will geometrically add this dimension to the coordinate system by transforming it, and we will see that both possible arrangements occur simultaneously. We now enter the box.

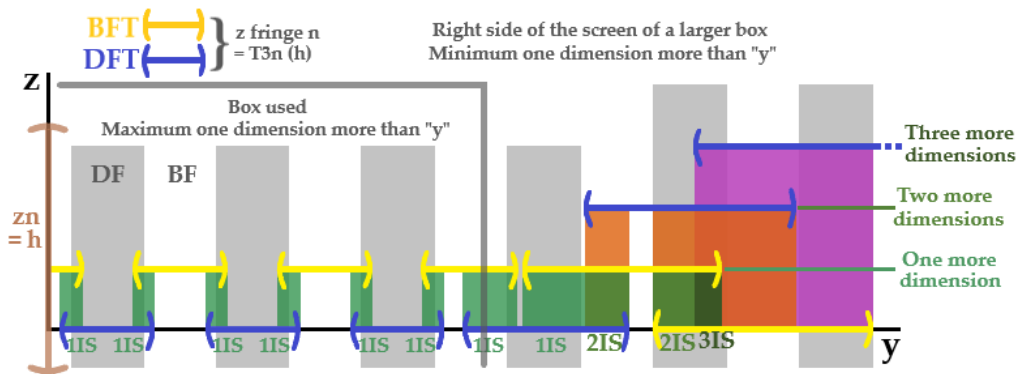


Figure 6. IS: Incompatible Space; DF: Dark Fringe; BF: Bright Fringe; DFT: Dark Fringe Trajectory; BFT: Bright Fringe Trajectory. In the diagram, the DFTs are prioritized along the y-axis. To eliminate ISs, the number of additional dimensions required on the screen (beyond “y”) depends on the number of ISs present along “y”. Large box: the minimum number of ISs along “y”, whether overlapping or not = 1; box used: the maximum number of ISs along “y” = 1; i.e. one additional dimension beyond “y” is needed on the screen

4. Passage in 4d — Figure 7

Since we have defined the 2d (y, x) where “x” represents the slit-screen dimension and “y”, represents the screen dimension, the only way to resolve these cases is to separate shadow and light within this 2d at phase 1 using parameters specifically set for box space, i.e. two shadow parameters, SP – the propagation of shadow in “x” and SM – the movement of shadow corresponding to the trajectories of dark fringes in “y”, and two light parameters, LP – the propagation of light in “x” and LM – the movement of light corresponding to the trajectories of bright fringes in “y”. At phase 2, we introduce an additional dimension, “a”, which is positioned coincident with “y”, and shares the same orientation. Then, at phase 3, we perform a horizontal transformation of the 2d (a, z). At phase 4, we transfer either SP and SM (case 1) or LP and LM (case 2) into this 2d (a, z). Following the standard method of adding a dimension in the horizontal plane, once “a” is added orthogonally to “y”, we obtain at phase 5: the 4d/4p 1 coordinate system (case 1) or the 4d/4p 2 coordinate system (case 2). Each of these systems eliminates incompatible spaces, as SM and LM now exist in different dimensions. However, both remain observationally incomplete as Case 1 contains only light propagation in “x”, allowing it to display only bright fringes, and Case 2 contains only shadow propagation in “x”, allowing it to display only dark fringes. To construct a single, observationally complete coordinate system, we need both LP and SP in “x”. However, merging these two 4d/4p coordinate systems presents a challenge: since each one evolves independently from the initial 3d reality, the merged system does not remain continuous with the starting reality—it appears duplicated. Furthermore, when we merge these systems at phase 6 and then transform this merged coordinate system by rotating the 2d (a, z) in the opposite direction, we find that phase 7 is structurally identical to phase 4 but now merged. Ideally, we should be able to transition directly from phase 3 to this merged phase 7, but due to the transfer process, this is not possible—the number of parameters doubles after merging. Despite this, we can still validate the merger after transfer by validating phase 7 in the transfer process. This is done through a technique called “copy-cross”, which allows us to transition from phase 3 to a new phase 7 within a 4d reference frame that remains geometrically compatible with the transferred phase 7. This validation is achieved using the rule of geometry limitation of links between parameters. In practice, we replace the original phase 7 (with its transfer parameters and output links) with the new phase 7. This new phase 7 retains parameters identical to the transfer parameters of phase 3 (the copy-cross parameters) but replaces output links with internal links, constructed within this new phase 7 and restricted by phase 3 to match the original transfer output links.

To allow alternating between transfer parameters and copy-cross parameters from phase 3 onward, we assign a number to all parameters starting at phase 4. In phases 1, 2 and 3: LP and SP are geometrically linked in “x” by an internal link and LM and SM are geometrically linked in “y” by an internal link. Transfer from phase 3 to phase 4: Once the parameters are moved from (y, x) and positioned in (a, z) at phase 4, each parameter is assigned a case number. Each case has two output links, resulting in a total of four output links (two per case). Phase 7 retains this same configuration, meaning it also contains transfer parameters and four output links. Copy-cross from phase 3 to the new phase 7: The parameters from (y, x) are copied into (a, z), or alternatively, parameters from an external contribution that function identically to these copies are used. Once these parameters are positioned in (a, z) in the new phase 7, the reference frame shifts to 4d. To align with the transfer phase 7, the parameters are numbered, and the links are crossed: since “x” coincides with “z” and “y” coincides with “a” the four internal links of the four dimensions “x”, “y”, “z”, “a” are arranged so that one dimension retains a parameter of one color while taking the parameter of the other color from the coincident dimension. Dimensions assigned a color in phase 4 (one parameter per dimension) form a link of the same color as the parameter retained. This results in two L links or two S links between “x” and “z” on the left and two L links or two S links between “y” and “a” on the right. Since phase 3 allows choosing between a phase 7 with output links and a new phase 7 with internal links, the limitation rule restricts the obtained links to output links, meaning the constructed 4 internal color links in the 4d reference frame of the new phase 7 are limited by the 3d to match the transfer output links. This limitation rule is effective because, first, it validates the obtained links. Second, limiting internal links to output links ensures that internal links are restricted to output links, keeping the parameters and fringe trajectories of different colors isolated across different dimensions, thereby eliminating incompatible spaces. The merged dimensions are “emptied of their geometric content”. Third, the links obtained function as full-fledged geometry links, preserving the relationships between parameters, dimensions, and transformation planes from the original 3d setup. These links are called 4d L or S links. Fourth, since the new phase 7 is geometrically unified with the transfer phase 7 via this limitation rule, the technique is validated. The copy-cross parameters and the 4d L or S links are then distributed to the new phases 6, 5, and 4 in the 4d reference frame. The internal links of the 3d, which are disregarded by the dimensions of the 4d reference frame during the copy-cross process, are referred to as “forgotten links” (these dimensions use the transfer process to contact 3d). Fifth, as the new phase 7 of the 4d reference frame is directly derived from phase 3 and the starting 3d, the merged 4d reality at the new phases 7 and 6 remains continuous with the starting reality of phases 1, 2, and 3. By unmerging the new phase 7 into the new phase 4, we separate this 4d reality into two 4d sub-realities connected by an “and” condition, each labeled as case 1 or 2, as assigned during the copy-cross. Sixth, since the reference frame for the observable horizontal field was validated in the new phase 6, it was already present in the starting reality, allowing us to determine the exact origin of the 4d parameters of (a, z). Transitioning from phase 3 to the new phase 7 (and indirectly to the new phase 4), we do not directly copy the parameters of (y, x) into (a, z). Doing so would simply duplicate parameters that are already present. Instead, parameters from an external contribution are used, which function identically to these copies. This means that, in addition to the 3d parameters, the technique introduces new parameters that come directly from 4d space. Moving from the new phase 7 to the new phase 8, we uncover a new property of the dimensions. Observing the two 4d L or S links between “y” and “a”, we lift the plane (a, z) at a right angle with the plane (y, x) returning to a 3d-shaped box space. Each of these links maintains the same right angle between the planes, directly between the dimensions. This defines two pivots at right angles between “y” and “a”. Since one link originates from “y” and the other from “a”, we can determine their directions. The “y” link, makes “y” experience the pivot, and the “a” link, makes “a” experience the pivot.

$$\text{Pivot “y” with respect to “a”} = \pi/2$$

$$\text{Pivot “a” with respect to “y”} = \pi/2$$

In this 4d coordinate system represented in 3d form, the right angle remains the same for one or both pivots, meaning that “a” is orthogonal to “y” through two pivots of $\pi/2$. For “x” and “z”, since we introduce a right angle between them when lifting the 2d (a, z), this forms a simple right angle between dimensions. However, similar to the pivots, this right angle can be subdivided into two right angles formed by the planes (y, x) and (a, z) directly connecting “x” and “z”. In the 4d coordinate system in 3d form of new phase 9, which summarizes all the right angles, we count right angle 1 from the 2d (y, x), right angle 2 of the 2d (a, z), right angle 3 between the dimensions “x” and “z”, and right angle 4 from the two pivots between “y” and “a” i.e.:

$$\text{“x” orthogonal to “y” orthogonal to “a” orthogonal to “z” orthogonal to “x”}$$

The particularity of coordinate systems 8 and 9 is that, due to the orthogonality between “y” and “a”, we cannot define the orthogonalities between “x” and “a” or between “y” and “z” unless we transition back to 3d. This return to 3d brings us back to phase 2, where we can confirm that the additional dimension is truly orthogonal to

the other three when transitioning to 4d. In this process, we use 3d to determine the positions of the axes, particularly ensuring that “y” and “a” remain coincident. Then, in 4d, where “y” and “a” are fundamentally orthogonal, we establish all the necessary orthogonalities:

“x” is orthogonal to “a” and “y” is orthogonal to “z” in 3d; “x” is orthogonal to “y”, “a” is orthogonal to “z” and “z” is orthogonal to “x” in 3d and 4d; and finally we place ourselves in 4d with “a” orthogonal to “y”.

In the Euclidean space, this confirms that the additional dimension is properly added orthogonally to the other three within the 3d coordinate system. The transformation of the 3d Euclidean vector space into a 4d coordinate system—formed by two orthogonal planes—is consistent with the scalar product and remains valid within the Euclidean space. Although the merged dimensions of the 4d reality remain compatible outside the box (since they were initially defined in 3d for the entire experiment space), they originate from the merging of dimensions that were each assigned a box space parameter at the 4d sub-reality level. This implies that the 4d coordinate system in 3d form is fundamentally a coordinate system of the box space itself. Regarding the incompatible spaces observed in 3d along “y”, one can simply transition to 4d to eliminate them. The T3n (h), which describe the horizontal trajectories of the fringes, are directly accounted for by the light and shadow parameters of “y”. These parameters are geometrically linked to the shadow and light parameters of “a”, ensuring that no incompatible spaces are created, as the overlapping spaces exist neither in “y” nor in “a”. Finally, an interesting aspect is the pseudo-3d space of phase 11, which represents a 4d coordinate system in 3d form but without the parameters of (a, z). Within this pseudo-3d space, the “forgotten links waiting for 4d color” remain ready to accommodate these parameters. The pseudo-3d space is particularly useful for easily visualizing the underlying dimension “a” within the observed space.

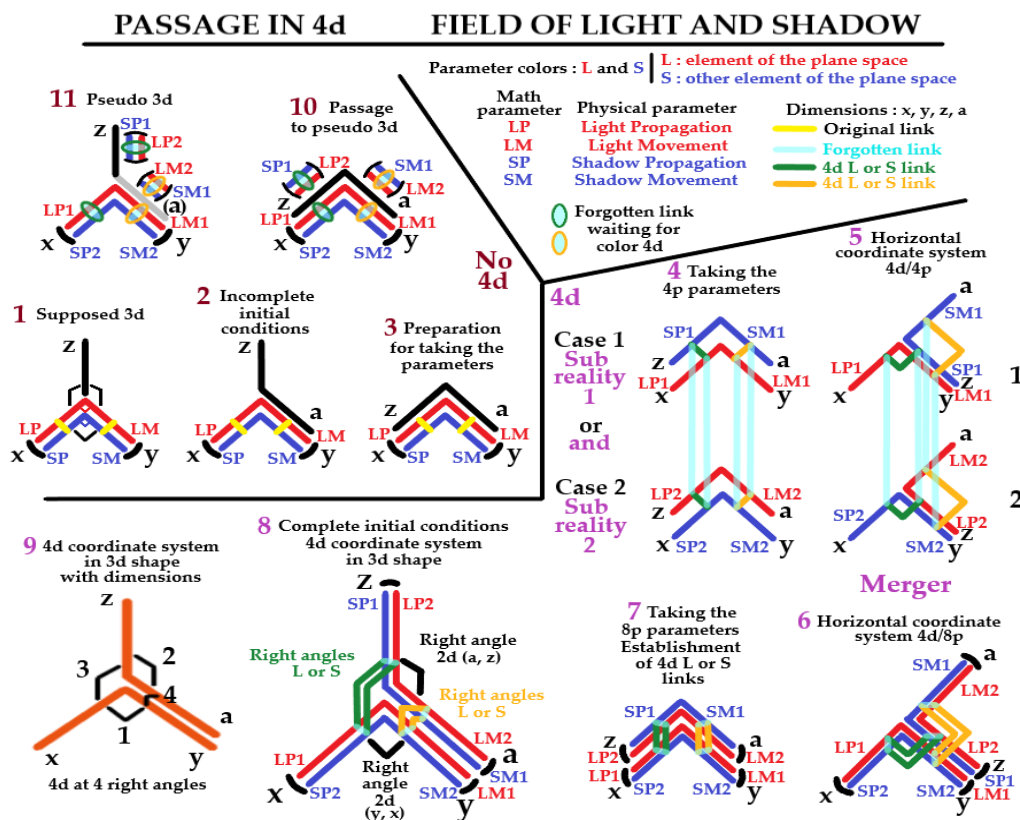


Figure 7. Transfer phases 4 to 9 resemble 4d phases, except that they involve transfer parameters and output links instead of the 4d L or S links. Additionally, their phase numbers are marked with a colored “No 4d” label. In 4d, we transition directly from phase 3 to the new phase 7 by revealing the 4d parameters of (a, z) and the 4d L or S links. These links establish contact with 3d, as they are restricted to the output links of the transfer. Furthermore, the key 4d properties introduced include the discontinuity in the propagation of the horizontal field in the new phase 6 and the presence of two right-angle pivots between “y” and “a” in the 4d coordinate system, which appears in 3d form in the new phase 8

5. Field and Photon

We obtain the spatial dimensional characteristics of both the horizontal field and a photon within the 4d reality of the box. The two 4d/4p coordinate systems, corresponding to the 4d sub-realities in the new phase 5, are merged into an observationally complete 4d/8p coordinate system of the horizontal field in the new phase 6. This system provides the characteristics of an observable photon, defined by $E=hC/\lambda$ at a specific point in the horizontal field. The photon itself is structured within four dimensions and eight parameters (4d/8p) and is made of two 4d/4p sub-parts, each consisting of one 2d light and one 2d shadow.

6. Discontinuous Propagation

Observing the image of the fringes, we notice that zSP1, positioned on the screen within the 4d/8p coordinate system of the new phase 6, represents a discontinuous propagation of shadow due to its orthogonality with LP1 in “x”. This means that shadow propagates along the screen only where it is visible, specifically at the dark fringes. Similarly, zLP2, also positioned on the screen within the same coordinate system, represents a discontinuous propagation of light due to its orthogonality with SP2 in “x”. This implies that light propagates along the screen only where it is visible, specifically at the bright fringes. From this, we obtain a fundamental property: zSP1LP2 is a “double discontinuous propagation of light and shadow observed on the screen”. This property is particularly interesting because it suggests the possibility of creating localized pieces of light and shadow, stopped or suspended in space, similar to holograms, by leveraging the field of light and shadow and its underlying geometry Figure 8.

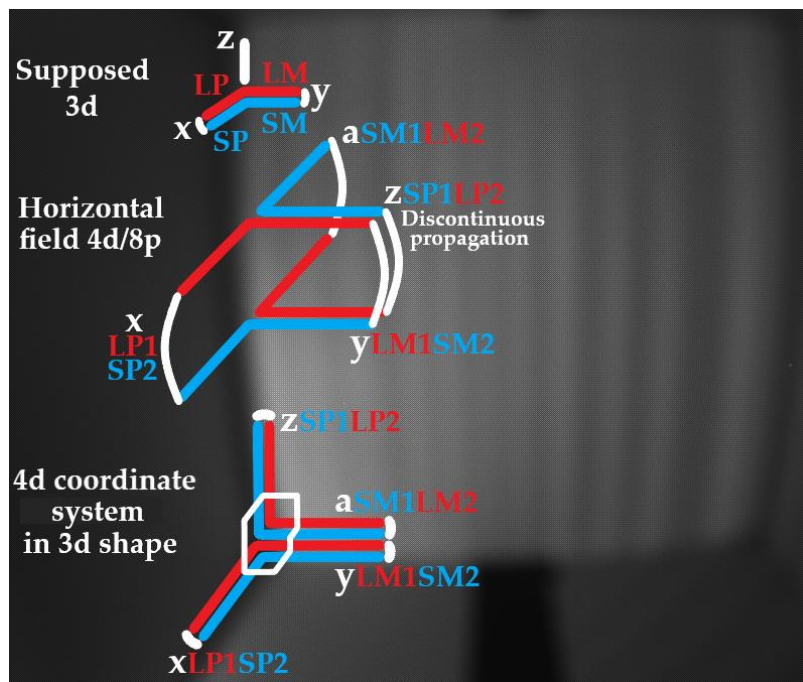


Figure 8. The supposed 3d, the horizontal field 4d/8p, and the 4d coordinate system in its 3d form are positioned on the fringe image. The slit is aligned with the extension of “x”. Within the horizontal field, the discontinuous propagation zSP1LP2 is visible on the screen

7. The Experience Is Just Beginning

By using a smaller box that allows a slight amount of brightness from the field to enter, either positioned over an eye or equipped with a camera, we observe light propagating in the darkness of the box in the form of small luminous discs. Among the notable observations already made, one of the most intriguing is the “hole in reality”—a phenomenon where one of these luminous discs transforms into the image of a specific area of 3d space located within the field but viewed from a position different from the actual observation point. This effect creates a directly observable spatial shortcut, which could be useful, for example, for viewing areas hidden by 3d relief Figure 9. Beyond this, the field of light and shadow also exhibits a remarkable compatibility with the

observer's perception and thought process. Its discovery marks the beginning of a new, more natural approach to physics.

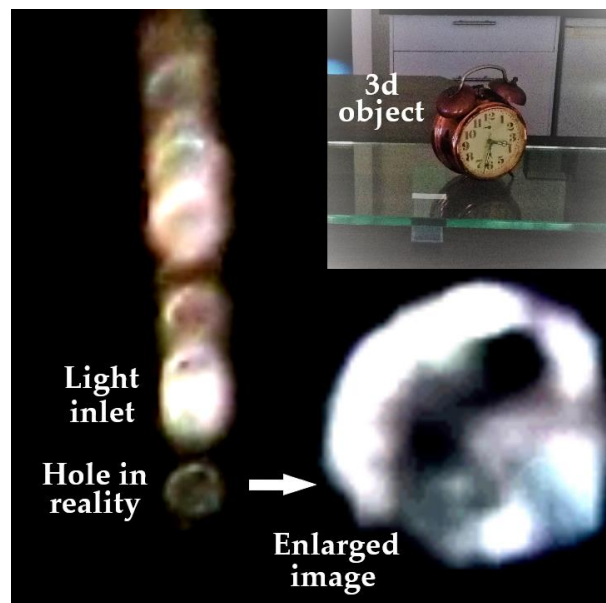


Figure 9. An image of a “hole in reality” is obtained using a camera with a small, drilled box placed over the lens. The light source is equipped with a bulb containing a single vertical filament. The brightness of the field entering the box reconstructs the image of a 3d object located within the field

8. Conclusion

This discovery reveals a field of light and shadow with novel spatial properties. When a nearly spherical light source—composed of vertical bands—diffuses its brightness throughout a room, bright and dark vertical fringes become visible on a screen inside a box equipped with a vertical slit. Remarkably, when the source is tilted, the fringes remain vertical, thereby challenging the validity of conventional 3d space. Since the fringe screen geometry requires the addition of exactly one dimension to restore spatial consistency, a 4d coordinate system specific to box space is constructed. This 4d system, valid within Euclidean geometry, reinterprets two dimensions that were coincident in 3d space as orthogonal when pivoted into 4d space. The resulting 4d Euclidean coordinate system constitutes an enhancement of the traditional four-dimensional \mathbf{R} -vector space, as all four dimensions are explicitly defined and characterized: they are emptied of their geometric content and assigned with light and shadow parameters adapted to real space. Within this four-dimensional box reality, it becomes possible to derive the full geometric characteristics of an observable photon, along with a discontinuity in the direct propagation of light and shadow through space. The field of light and shadow thus emerges as an independent experiential domain. Since the 4d reality of this field diverges from the familiar 3d reality, a conceptual adaptation is necessary to reconcile it with existing three-dimensional frameworks. These initial properties may lead to a wide range of potential applications.

Acknowledgments

Thanks to computer support J2M, and English-proofreading-experts for improving the manuscript.

Authors' contributions

As a single author, I have read and approved the final manuscript.

Funding

There was no funding.

Competing interests

The author declares that he has no known competing financial interests or personal relationships that could have appeared to influence the work reported in this paper.

Informed consent

Obtained.

Ethics approval

The Publication Ethics Committee of the Canadian Center of Science and Education.

The journal and publisher adhere to the Core Practices established by the Committee on Publication Ethics (COPE).

Provenance and peer review

Not commissioned; externally double-blind peer reviewed.

Data availability statement

The data that support the findings of this study are available on request from the corresponding author. The data are not publicly available due to privacy or ethical restrictions.

Data sharing statement

No additional data are available.

Open access

This is an open-access article distributed under the terms and conditions of the Creative Commons Attribution license (<http://creativecommons.org/licenses/by/4.0/>).

Copyrights

Copyright for this article is retained by the author(s), with first publication rights granted to the journal.

References

- Bellavitis, G. (1835). *Annali delle Scienze del Regno Lombardo-Veneto* (vol. 5). “Saggio di applicazione di un nuovo metodo di geometria analitica” section, p. 244-259.
- Bolzano, B. (1804). *Betrachtungen über einige Gegenstände der Elementargeometrie*.
- Cayley, A., & Forsyth, A. R. (1889-1897). *The collected mathematical papers of Arthur Cayley* (vol I). “On a Theorem in the Geometry of Position” section.
- Chasles, M. (1837). *Aperçu historique sur l'origine et le développement des méthodes en géométrie*.
- Clifford, W. K. (1878-1887). *Elements of Dynamic*.
- Dahan-Dalmedico, A., & Peiffer, J. (1986). *Une histoire des mathématiques*. Routes et dédales, chap. 4.
- de Fermat, P. (1662). *Synthèse pour les fractions*.
- de Fermat, P. (1679). *Ad locos planos et solidos isagoge*.
- Descartes, R. (1637). *Discours de la méthode*.
- Descartes, R. (1637). *La Géométrie*, LIVRES I, II, III.
- Dimensions et paramètres-Physique, n.d., Web page.
- Einstein, A. (1905). *Annalen der Physik* (vol. 322). “Über einen die Erzeugung und Verwandlung des Lichtes betreffenden heuristischen Gesichtspunkt” section.
- Euclid, 3rd century BC, *Elements* (Στοιχεῖα / stoikheia).
- Fascicule CNED de Physique-Corpusculaire. Préparation au Concours EMA 2005, January 2004.
- Gottfried Wilhelm von Leibniz is the originator of the word “coordinate”, as cited in: H.S.M. Coxeter, 1961, *Introduction to Geometry*, “8. Coordinates” section.
- Hermann Grassmann, 1844, *Ausdehnungslehre*.

Laguerre, E. N. (1898-1905). Œuvres complètes, tomes 1 et 2.

Möbius, A. F. (1827). Der barycentrische Calcul: ein neues Hilfsmittel zur analytischen Behandlung der Geometrie.

Newton, I. (1687). Philosophiæ Naturalis Principia Mathematica.

Newton, I. (1730). Opticks: or, a treatise of the reflections, refractions, inflections and colours of light, the fourth edition, corrected.

Peano, G. (1888). Calcolo geometrico secondo l'Ausdehnungslehre di H. Grassmann preceduto dalle operazioni della logica deduttiva.

Poncelet, J.-V. (1822). Traité des Propriétés Projectives des Figures, rééd. Jacques Gabay, 1995.

William Rowan Hamilton introduced quaternions in 1843, In T. L. Hankins, Sir William Rowan Hamilton (1980).

Young, T. (1804). Experiments and Calculations Relative to Physical Optics.